Edinburgh, Scotland
EURONOISE 2009
October 26-28

Assessment of jet noise shielding prediction parameters

Ciarán J. O'Reilly[a]
Henry J. Rice[b]
Department of Mechanical and Manufacturing Engineering, Trinity College Dublin, Ireland

ABSTRACT

Positioning aircraft engines on the rear of the fuselage above a U-shaped empennage is a concept configuration, which is expected to reduce the engine noise propagated towards the ground during take-off and approach. In order to assess the noise reduction benefits attainable from such a configuration, it is necessary to firstly develop appropriate acoustic evaluation tools. In this paper, a new methodology is presented, which uses a RANS solution input to model the complex jet flow as acoustic sources for use in shielding predictions. This methodology is employed as a sensitivity analysis tool in order to establish which parameters are important to consider in jet shielding predictions. Although, the predicted isolated jet directivity agrees well with far-field empirical values, the predicted levels of shielding are much larger than those observed in the available data. A preliminary investigation into the possible causes of this discrepancy indicates that the introduction of the shield adjacent to the jet results in the generation of new `installation' sources, which limit the shielding achievable in practical applications.

1. INTRODUCTION

Reducing the noise generated by aircraft on takeoff and approach is an essential consideration in the design of new commercial aircraft[1]. A novel approach to reduce the jet noise from aircrafts that propagates towards the ground, currently under consideration as part of the European FP6 Project 'New Aircraft Concepts Research' (NACRE), is to position the engines high on the rear of the aircraft fuselage, so that a new U-shaped empennage design, would potentially act as a noise shield or barrier. Design evaluation tools must be developed which can evaluate such shielding configurations within the time and computational constraints of industry.

To date, the acoustic benefit of such a configuration has been quantified by the insertion loss or shielding factor, which is the decibel difference between the installed and isolated jet sound pressure level at a far-field receiver. As the majority of jet noise research conducted over the past sixty years has focused on isolated jets, it is unclear which traditional jet model parameters are important when it comes to the prediction of the shielding factor. In this present paper some parameters believed to be relevant are examined with the aim of guiding future investigation in this area.

2. ACOUSTIC PREDICTION METHODOLOGY

The Tam-Auriault jet noise prediction method has been shown to agree well with a wide set of jet noise data[2]. This apparent improvement over traditional Lighthill based predictions may possibly be attributed to the fact that it is a derivative of the source, which is modelled in the cross-correlation, as opposed to the source itself in traditional Lighthill models[3]. Instead of following traditional Lighthill based methods, the Tam and Auriault approach is adopted in order to retain an explicit Green's function term in the spectral density expression. This Green's function may subsequently be modelled to include a scattering object.

[a] Email address. cjoreill@tcd.ie
[b] Email address. hrice@tcd.ie

$$\frac{\partial^2 \rho'}{\partial t^2} - c_0^2 \nabla^2 \rho' = \frac{\partial^2 T_{ij}}{\partial x_i \partial x_j} \tag{1}$$

The Lighthill model may be derived to use the same type of correlation model as the Tam and Auriault model, if one derivative in the source term of Lighthill's equation (equation 1) is transferred to the Green's function through integration-by-parts, while the other is retained on the source. Although this transfer is arbitrary, it may possibly improve jet noise predictions. Therefore, the far-field space-time density fluctuations, ρ', may written as

$$\rho'(\mathbf{x},t) = -\frac{1}{c_0^2} \int\int\int \frac{\partial \mathbf{G}}{\partial x_{\mathbf{s}i}}(\mathbf{x},\mathbf{x_s},\omega) \frac{\partial T_{ij}}{\partial x_{\mathbf{s}j}}(\mathbf{x_s},t_s) \exp\left(-i\omega(t-t_s)\right) d\omega\, dt_s\, d\mathbf{x_s} \tag{2}$$

where $\mathbf{G}$ is a frequency domain Green's function, T_{ij} is the Lighthill stress tensor, c_0 is the ambient speed of sound and the subscript $\mathbf{s}$ denotes at the source position.

To simplify the analyses, the shear-noise terms in the correlation are neglected and the various i and j components of this equation are replaced by a single component in the direction of the receiver, as shown by Proudman[4], The spectral density of the radiated sound may be expressed as

$$\begin{aligned} S(\mathbf{x},\omega) = \int\cdots\int & \frac{\partial \mathbf{G}}{\partial x_{\mathbf{1}r}}(\mathbf{x},\mathbf{x_1},\omega) \frac{\partial \mathbf{G}}{\partial x_{\mathbf{2}r}}(\mathbf{x},\mathbf{x_2},\omega) \left\langle \frac{\partial T_{rr}}{\partial x_{\mathbf{1}r}}(\mathbf{x_1},t_1) \frac{\partial T_{rr}}{\partial x_{\mathbf{2}r}}(\mathbf{x_2},t_2) \right\rangle \\ & \times \exp\left(-i(\omega_1+\omega_2)t + i\omega_1 t_1 + i\omega_2 t_2\right) \delta(\omega-\omega_2)\, d\omega_1\, d\omega_2\, dt_1\, dt_2\, d\mathbf{x_1}\, d\mathbf{x_2} \end{aligned} \tag{3}$$

A correlation function is selected for the present model, which retains the shape of the function employed by Ribner[5], in a fixed reference frame

$$\left\langle \frac{\partial T_{rr}}{\partial x_{\mathbf{1}r}}(\mathbf{x_1},t_1) \frac{\partial T_{rr}}{\partial x_{\mathbf{2}r}}(\mathbf{x_2},t_2) \right\rangle = \frac{\bar{\rho}^2 \overline{u_t^2}^2}{l_t^2} \exp\left(-\frac{\pi \eta_1^2}{U_C^2 \tau_t^2} - \frac{\pi}{l_t^2}\left((\eta_1 - U_C \tau)^2 + \eta_2^2 + \eta_3^2 \right) \right) \tag{4}$$

Evaluating the frequency and time integrals in equation 3 (following the manipulation shown in Tam and Auriault's paper[2] leads to the far-field spectral density from an elemental volume as

$$\partial S(\mathbf{x},\mathbf{x_s},\omega) = \frac{\omega^2 l_t \tau_t 2\pi \bar{\rho}^2 \overline{u_t^2}^2}{c_0^2} \left| \mathbf{G}(\mathbf{x},\mathbf{x_s},\omega) \right|^2 \exp\left(-\frac{\omega^2}{4\pi}\left(C^2 \tau_t^2 + \frac{l_t^2}{U_C^2} \right) \right) \tag{5}$$

where l_t is the integral length scale, τ_t is the integral time scale, $\bar{\rho}$ is the mean density, and $\overline{u_t^2}$ is the turbulent kinetic energy. $C = 1 - U_C \cos\theta / c_0$ is a convection term where U_C the convection velocity and θ is the angle between source and receiver.

With the aid of a κ - ϵ Reynolds-averaged Navier Stokes (RANS) solution of the jet flow the remaining terms may be evaluated as

$$l_t = c_l\left(\kappa^{3/2}/\epsilon\right); \quad \tau_t = c_\tau(\kappa/\epsilon); \quad \overline{u_t^2} = c_A(2\kappa/3) \tag{6}$$

where c_l, c_τ and c_A are model constant, which are typically set using far-field spectral data. Upon evaluation of the Green's function in equation 5 for installed and isolated jet configurations, the shielding factor may be determined. For more details see reference 6.

3. ACOUSTIC PREDICTIONS

A number of predictions have been made on the coaxial jet and 2D profile aerofoil shield (EUROPIV) used in the NACRE test campaign. In this paper the predictions are compared against data which has been altered due to confidentiality requirements but which is still indicative of jet shielding measurements.

A. Source Location Effects

As the calibration of model constants, c_l and c_τ, changes the location of the modelled jet source, a comparison of the predicted (isolated and shielded) far-field values was performed between calibrated ($c_l = c_\tau = 0.3$) and uncalibrated ($c_l = c_\tau = 1$) sources.

Figure 1 shows the far-field SPL for the isolated configuration. The differences are relatively small, considering the large shift in axial position (as much as four diameters for the low frequency sources) and both sets of results match the data well. It could be claimed that far-field isolated predictions are relatively robust to variations in RANS input or source location, although this may be a little over-optimistic.

A note-worthy feature of the difference in directivity, resultant from the two different source locations, may be observed at 500Hz. Although the sources have been moved downstream in the calibration, towards the lower angled receivers, this prediction shows a lower directivity than the uncalibrated sources, when the opposite might be expected. This is because at the downstream location, the sources convect at a slower Mach number and are, therefore, less directional -- there is a trade-off between the source directionality and position. The implication of this is that, although c_l and c_τ may be *tuned* for different jet models or different RANS solutions, jet noise predictions will still be heavily influenced by spatial variations in the RANS variables.

Figure 2 presents the shielding factor for the two source locations, predicted using the Fresnel-Kirchhoff method (FKM)[6]. The EUROPIV (foil and flap) was approximated as a single flat surface. Unfortunately, there is poor agreement between the predicted shielding factors and the data levels. It will be shown in subsequent analyses that this disagreement between the predicted and measured shielding levels is observed throughout the prediction comparisons. However, some useful traits of the modelling methods may still be noted. A shift in source location has been accompanied by a complementary shift in shielding directivity, with peak levels remaining unchanged. This result highlights the importance of accurate source positioning to shielding prediction.

B. Mean Flow Propagation Effects

The jet self-noise sources, which have been considered in this work, are in themselves omni-directional. The directionality of the sound field generated by a jet is due to the mean flow (for the most part), which convects the sources downstream, and also refracts the propagating sound away from the axis.

The convection of the source by the mean-flow acts to amplify the source in the downstream direction and Doppler shifts the frequency of the propagating sound field. This convection effect has been included in the present model, through the correlation function and appears as the convection factor. In the evaluation of the convection factor, the convection velocity must be estimated, most likely, using a scaled function of space based on the axial velocity from the RANS solution[7,8]. However, different jet noise models, with varying model constants, can lead to very different jet source locations and, therefore, different underlying mean flow values for the source.

In order to assess the impact of source convection on shielding predictions, two cases were compared, namely, with and without source convection. Figure 3 present the far-field acoustic predictions for this comparison. It can be observed that there is a shift in the angle of peak shielding (certainly at lower frequencies), and also, an increase in the shielding factor when the sources are omni-directional. It is reasonable to expect that these trends should also be observed at other convection values.

The refractive effect of the mean jet flow on sound propagation has been included through a directivity correction factor (see reference 6). This is very much an approximate approach but it should be sufficient to identify whether or not refraction is a likely to be responsible for the large differences between the predicted shielding levels and the data values. Figure 4 shows the shielded predictions. The results with refraction only show a small deviation from those without refraction. Although it is difficult to draw any clear conclusions, as the margins of difference are quite small, it may be said that refraction of the propagating sound does not appear to be reason for the large differences between predicted shielding factors and the test data.

4. A LACK OF SHIELDING?

Perhaps the most striking feature of available data is the low shielding levels (a 4dB reduction at most) even at the highest frequencies. For an incoherent source distribution, positioned near the location of the secondary nozzle lip, shielding factors of up 20dB are predicted, as shown in figure 5. This magnitude of attenuation is typical of predictions for computational setups of this type (as has been shown in references 9 and 10 amongst many others). Although there may be some uncertainty as to the location of low-frequency jet noise sources, it can be expected that high-frequency jet noise production is concentrated in the shear layer immediately downstream of the nozzle lip. There are a number of possible reasons why these methodologies fail to predict the observed levels of shielding.

A. The Role of Jet Noise Models

Lighthill's equation is exact. The problem with acoustic analogies is not so much the analogies themselves, but rather the inexact flow information they rely upon. Steady-state RANS solutions provide limited averaged information about jet flow fields, and are themselves subject to significant variations, which impact the accuracy of acoustic predictions.

Using time-averaged inputs to acoustic analogy type models requires the modelling of space-time correlation functions, which scale over the source region. A great variety of models have been proposed since Lighthill's papers in the early 1950s, which attempt to match the turbulent statistics within the source region, and ultimately enhance far-field spectral and directivity predictions. A RANS solution may be used to provide the necessary amplitude values for these functions, however, due to the inaccuracies of RANS solutions, it is also necessary to calibrate the jet noise model inputs, through model constants. As vast databases of local turbulent properties, for a wide range of nozzles and flow conditions, do not exist (and are indeed impractical), calibration is based on far-field spectra or directivity.

Such calibration of statical flow properties shifts the jet source region, and therefore, the source location is effectively driven by far-field values in order to compensate for the deficiencies in the RANS solution. The true *predictive* ability of RANS dependent jet models must be questioned. It could be argued that such models are, in a sense, more of an interpolation method for use with far-field databases, and it may be more logical to simply interpolate the databases directly.

Even if RANS dependent models are acceptable for far-field isolated predictions, their inherent source-location uncertainty (at least at low frequencies) is more of an issue when an acoustic shield, located in the near-field, is of interest. The direction of peak shielding is quite sensitive to the location of the equivalent jet noise sources. That said, however, a shift in source location still does not explain the over-prediction in shielding levels, although it is important to consider its influence on predictions, as in case of comparing different shielding predictions from different jet models.

For high-frequency jet noise, the problem is somewhat less ambiguous, as regardless of the jet noise models, it can be expected that the equivalent source region is adjacent to the nozzle exit. Different noise models, may predict different noise directivity patterns, however, it would appear that the directivity of the jet noise is not overly important to shielding predictions -- at least not as much as source location.

The disagreement of the model predictions with the test data can not simply be attributed to the particularities of the jet models. However, the assumption that equivalent jet sources could be evaluated from the isolated mean flow profile may still be erroneous.

B. Alternative Propagation Paths

It has been assumed in this present work that the shielded noise has not been reflected by other objects present in the tests back towards the far-field receivers. This assumption neglects the potential of the large nozzle body to influence the acoustic field. Jet noise impinging on the nozzle directly will not have a significant influence on the shielding effect, as the nozzle is present in both the isolated and installed configurations. If anything it should lead to increased

shielding levels, as a source will appear to be located directly over the shield. However, sound, which has been scattered back from the upper surface of the shield, may be reflected by the nozzle body towards the far-field receivers once more. It may also be the case that the Fresnel-Kirchhoff method (FKM) shielding predictions over-simplify the shield geometry (as the FKM can only consider flat surfaces as shields). Figure 6 shows the nozzle and EUROPIV shield locations, as they have been included in a 3D numerical computation, and a comparison of the shielding factors obtained from a single 4kHz monopole point source located on the jet axis above varying shield geometries. As can be observed the aerofoil and flap does not achieve the levels of shielding predicted for a flat surface, however, this loss in shielding is still not comparable with the test data, and high shielding levels are expected directly below the shield. It must also be remembered that the approximation of the aerofoil as a flat surface is more appropriate at higher frequencies than that computed here, and therefore, the difference observed here is expected to be less at higher frequencies.

Also in figure 6, are shielding predictions that include the side-plates and side-beams (the full EUROPIV), and the nozzle body. These have a relatively small impact on the predicted shielding level. It would, therefore, seem unlikely that the poor shielding levels in the test are due to the sound propagating to the far-field receivers by reflecting from objects not considered in the FKM predictions.

It could also be suggested that the unsteady turbulence itself reflects the sound back towards the receivers in the same manner as the nozzle body. Cerviño *et al.*[11] showed in their numerical perturbation simulations that some back-scatter may be observed from a sound waves impinging on unsteady vortex roll-up. However, given the limited effect on the shielding factor that multiple reflections off the nozzle body had, it would seem extremely unlikely that any reflections off the turbulence would have the amplitude to play a significant role in the test.

C. Shield Generated Flow Noise

The EUROPIV shield was possibly located close enough to the jet to interfere with its flow entrainment. Figure 7 shows a 2D RANS solution for the configuration under investigation. It can clearly be observed that the flow increases in velocity across the top surface of the shield due to entrainment by the jet. A typical entrainment velocity profile, for an isolated nozzle, is still evident at the top lip of the nozzle.

Of greater relevance to present question is that, it is indicated in this figure, from the turbulent kinetic energy, that a source may be generated at the leading-edge of the EUROPIV and also at the trailing-edge of the main foil. It is acknowledged that the 2D nature of this computation may exaggerate such an effect, and it is difficult to estimate the relative amplitude of a leading-edge source. As an initial indication of the impact that a source in this location may have on the shielding factor, an additional isolated source is added at the leading edge location in the predictions. The source strength here is just one-percent of the total source amplitude for each frequency. This is an unrealistic source as any noise generated by this mechanism would vary in location for different frequencies but it does help illustrate the point. It may seen that a considerable loss in shielding is predicted. Although this computation is quite crude, and has also changed the direction of peak shielding, it does show that any source with a clear line-of-sight to the far-field receivers would have a considerable impact on the shielding levels.

In his 1981 paper, Wang[12] examined experimentally the effects of the wing on jet noise propagation for an under-wing installation. He states that "*the boundary layer generated on the surface of the wing as the result of entrainment of the air into the region between the wing and the jet is believed to be responsible for the low-frequency noise enhancement*".

In addition to this boundary layer noise, a trailing-edge source would contribute to increased high-frequency noise. It would, therefore, seem most likely that the inclusion of additional *installation* sources is responsible for the differences between predicted and test shielding levels. The shielding factor is sensitive to contamination from additional sources.

D. Near-Field Excitation

Tinney and Jordan[13] have recently described an evanescent acoustic field, which dominates measurements of the irrotational hydrodynamic periphery of (coaxial) jets. This field is driven by the large-scale turbulent structures. The existence this field has been recognised for some time, and as far back as 1960, Howes[14] discussed how a microphone in the near-field will be subject to fluctuations associated with incompressible ``pseudo-sound'', which does not propagate, and compressible propagating sound waves. However, there is no indication in the literature of how the insertion of an object in, or near, this field influences the far-field sound. Indeed, it should be remembered that there is no consensus on large scale jet structures themselves (see reference 15).

It is speculated that the presence of the EUROPIV in the NACRE test may have scattered some of these waves to the far-field. This effectively means that additional sources may be present, which have not been included in the present shielding methodologies. Once again, any additional small amplitude source, located in a disadvantages position, could be responsible for a dramatic reduction in shielding levels.

E. Back-Scatter Source Amplification

The location of the acoustic shield near to the jet may alter the jet source terms themselves. It may be possible that the back-scatter from the shield increases the term. Not only would this amplify the shielded source but may also change the source locations. As the order-of-magnitude of this effect in not available from the published literature, its influence on the measured shielding levels can not be assessed at this point.

5. CONCLUSIONS

- Present methodologies to predict the far-field shielding levels, from an installed jet configuration, fail to reproduce the test data values.
- Identification of source locations is critical to noise shielding predictions, whereas source directivity is mildly important.
- Although isolated far-field jet noise models may be relatively robust to the inherent deficiencies in RANS flow solutions, installed far-field predictions appear to be quite sensitive to these shortcomings.
- The unexpectedly low shielding levels, observed at high frequencies in the test data, are most likely due to near-field effects resultant from the introduction of the shield, which have not included in present shielding methodologies. The assumption that the noise source is the same for both the isolated and installed configurations is mostly likely invalid.

FIGURES

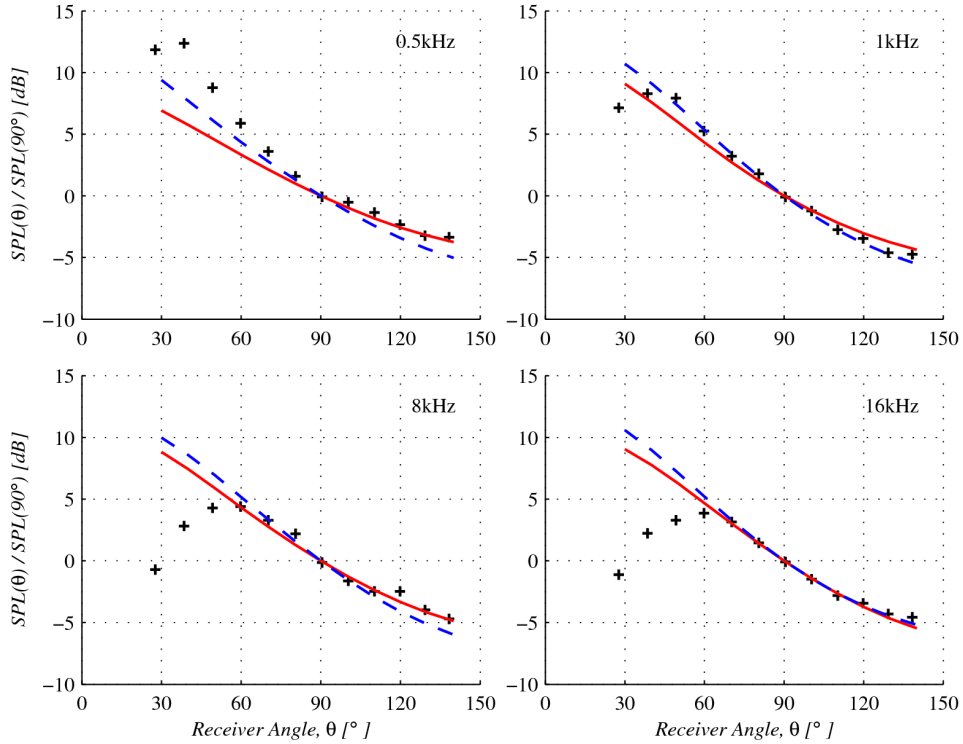

Figure 1: Axial source location: isolated normalised far-field SPL [dB] directivity from sample test data (black +) and predicted values with uncalibrated (blue --) and calibrated (red -) model constants.

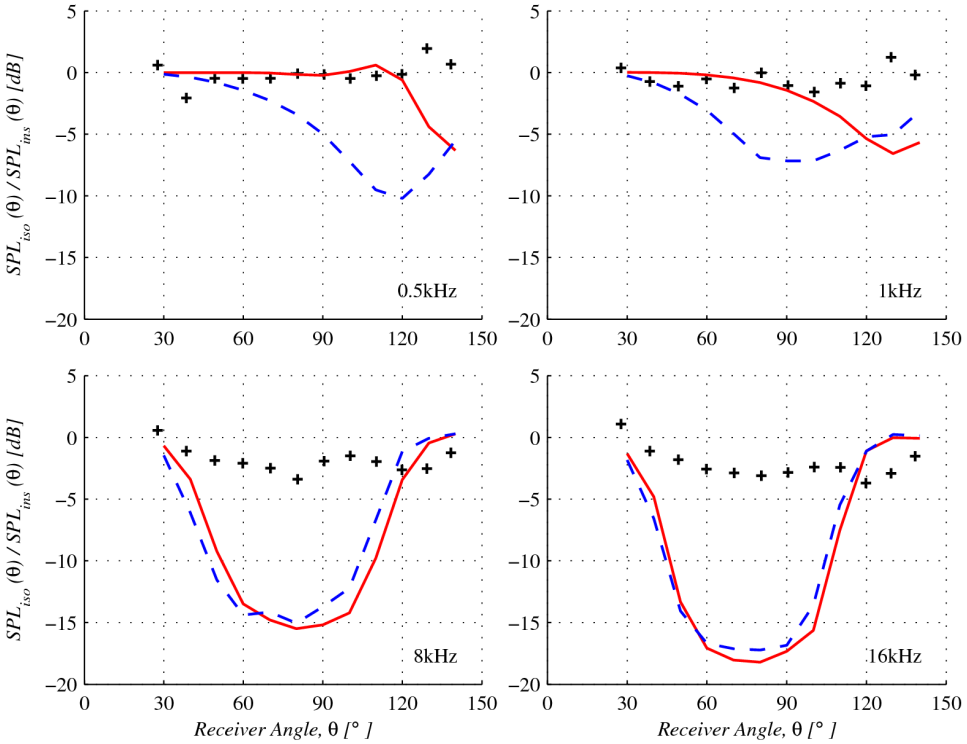

Figure 2: Axial source location: far-field shielding factor [dB] directivity from sample test data (black +) and predicted values with uncalibrated (blue --) and calibrated (red -) model constants.

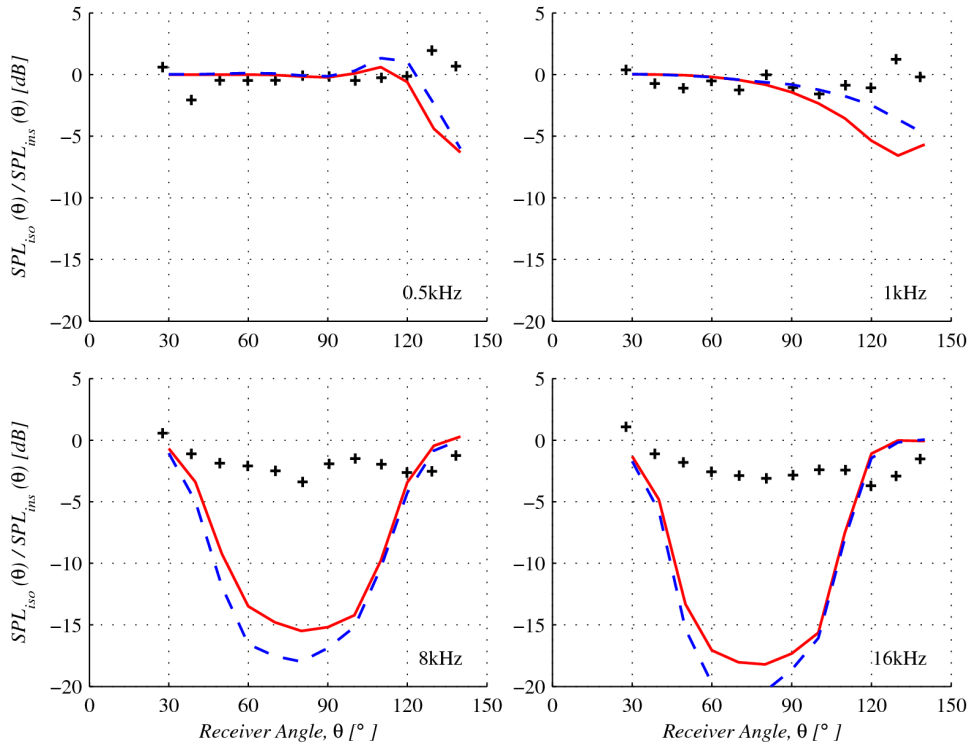

Figure 3: Source convection: far-field shielding factor [dB] directivity from sample test data (black +) and predicted values with convection (red -) and without convection (blue --).

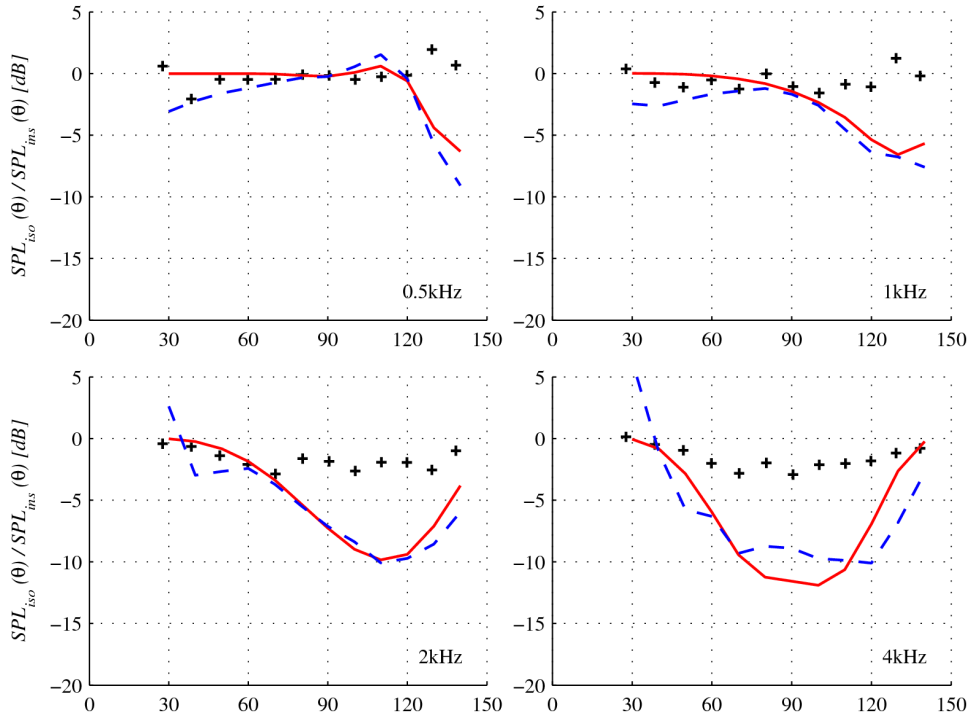

Figure 4: Flow refraction: far-field shielding factor [dB] directivity from sample test data (black +) and predicted values without (red -) and with (blue --) a refraction correction factor

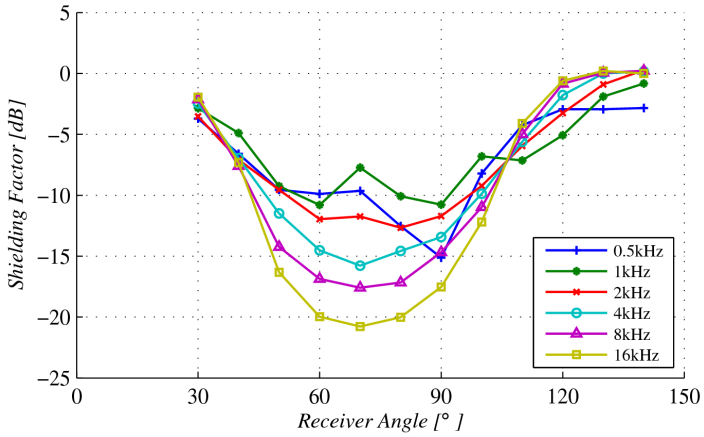

Figure 5: Shielding factor from a ring of incoherent monopoles on the secondary exit plane.

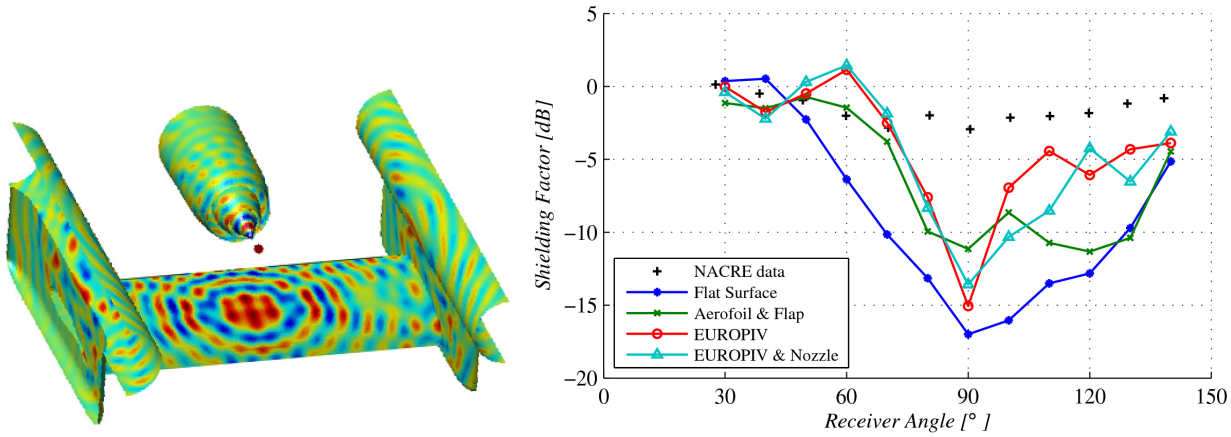

Figure 6: 3D numerical solution for a 4kHz monopole point source located on the jet axis over the EUROPIV with the nozzle present (left) and the shielding factors from a 4kHz monopole point source located on the jet axis above the shields / reflectors of varying complexity (right).

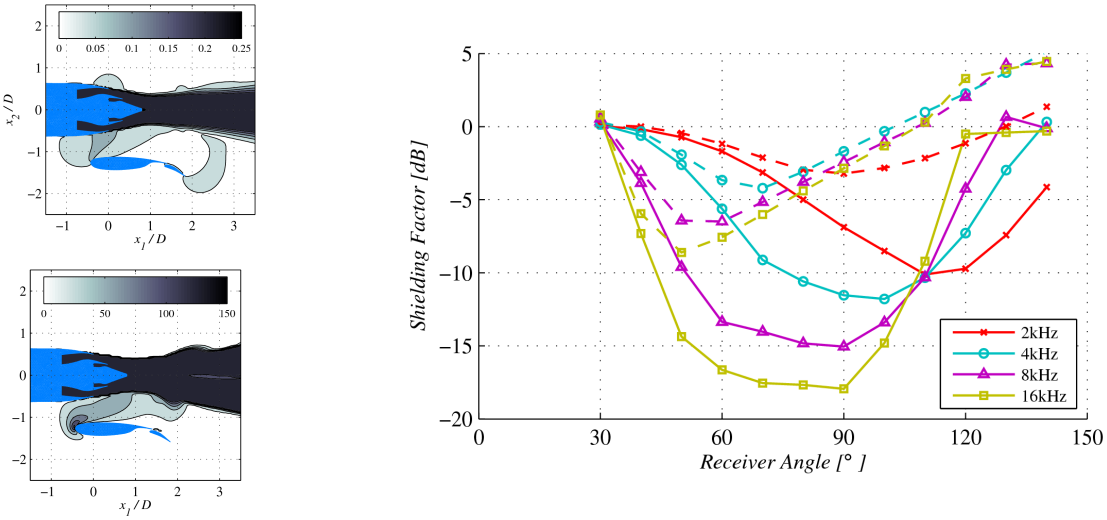

Figure 7: Shield generated noise: 2D RANS solution of the installed test configuration with Mach number (top-left) and turbulent kinetic energy [m^2/s^2] (bottom-left). Far-field shielding factor [dB] directivity with (--) and without (-) an isolated source at the leading-edge of the shield (right). The amplitude of this source is only one-percent of the total jet source model amplitude.

ACKNOWLEDGMENTS

The authors would like to thank the European Commission and NACRE project (contract no. AIP4-CT-2005-516068) partners for their funding and collaboration.

REFERENCES

1. R. J. Astley et al., “Predicting and reducing aircraft noise”, in *Proceedings of ICSV14*, Cairns, Australia, 2007.
2. C. K. W. Tam and L. Auriault, “Jet mixing noise from fine-scale turbulence”, *AIAA Journal* **37**(2), pp.145-153, 1999.
3. P. J. Morris and F. Farassat, “Acoustic analogy and alternative theories for jet noise prediction”, *AIAA Journal* **40**(4), pp.671-680, 2002.
4. I. Proudman, “The generation of noise by isotropic turbulence”, in *Proceedings of the Royal Society of London, Series A* **214**, pp.119-132, 1952.
5. H. S. Ribner, “Quadrupole correlations governing the pattern of jet noise”, *Journal of Fluid Mechanics* **38**, pp.1-24, 1969.
6. C. J. O'Reilly, “On the acoustics of installed subsonic jets”, PhD Thesis, University of Dublin, Trinity College, 2009.
7. P. A. O. L. Davies, M. J. Fisher and M. J. Barratt, “The characteristics of the turbulence in the mixing region of a round jet”, *Journal of Fluid Mechanics* **15**(3), pp.337-367, 1963.
8. W. Béchara, P. Lafon and C. Bailly, “Application of a κ - ϵ turbulence model to the prediction of noise for simple and coaxial free jets”, *Journal of the Acoustical Society of America* **97**(6), pp.3518-3531, 1995.
9. A. Agarwal, A. P. Dowling, H. Shin, W. Graham and S. Sefi, “A ray tracing approach to calculate acoustic shielding by the silent aircraft airframe”, in AIAA/CEAS 12th Aeroacoustics Conference (Cambridge, Massachusetts, USA), paper AIAA-2006-2618, 2006.
10. M. Lummer, “ Maggi-Rubinowicz diffraction correction for ray-tracing calculations of engine noise shielding”, *AIAA/CEAS 14th Aeroacoustics Conference (Vancouver, British Columbia, Canada)* paper AIAA-2008-3050, 2008.
11. L. I. Cerviño, T. R. Bewley, J. Freund and S. K. Lele, “Perturbation and adjoint analyses of flow-acoustic interactions in an unsteady 2D jet”, in *Center for Turbulence Research -- Proceedings of the summer program*, pp.27–40, 2002.
12. M. E. Wang, “Wing effect on jet noise propagation”, *Journal of Aircraft* **18**(4), pp.295-302, 1981.
13. C. E. Tinney and P. Jordan, “The near pressure field of co-axial subsonic jets”, *Journal of Fluid Mechanics* **611**, pp.175-204, 2008.
14. W. L . Howes, “Distribution of time-averaged pressure fluctuations along the boundary of a round subsonic jet”, *NASA Technical Note D-468*, 1960.
15. P. Jordan and Y. Gervais, “Subsonic jet aeroacoustics: associating experiment, modelling and simulation”, *Experiments in Fluids* **44**(1), pp.1-21, 2008.